Pergamon

Polyhedron Vol. 17, No. 23–24, pp. 4091–4099, 1998

0277–5387/98 \$19.00+0.00

PII: S0277–5387(98)00214–9

Persulfurated complexes of palladium(II) and platinum(II) with fluorinated aryl-thiolates. X-ray structure of $[Pt(SC_6F_5)_2(CH_3SCH(CH_3)CH(CH_3)SCH_3)]$

Erika Martin,*[a] Beatriz Toledo,[a] Hugo Torrens,[a] Fernando J. Lahoz[b]
and Pilar Terreros[c]

[a]DEPg., F. Química, UNAM, 04510, Mexico D.F., Mexico

[b]Depto. de Química Inorgánica, ICMA-CSIC, Universidad de Zaragoza, 50009 Zaragoza, Spain

[c]ICP-CSIC, Cantoblanco, 28049 Madrid, Spain

(Received 12 February 1998; accepted 21 May 1998)

Abstract—The syntheses of the persulfurated $[M(SR_F)_2(CH_3SCH(CH_3)CH(CH_3)SCH_3)]$, M = Pd or Pt; $R_F = C_6F_5$ or C_6F_4H-4 compounds allow the separation of two diastereomers and the NMR detection of five conformers (three *anti* and two *syn*) of each compound. ^1H, ^{19}F and ^{195}Pt NMR data have been used to assign each conformer and to obtain their relative populations as well as to follow their equilibrium at high temperatures. The X-ray diffraction molecular and crystalline structure of $[Pt(SC_6F_5)_2(CH_3SCH(CH_3)CH(CH_3)SCH_3)]$ has been determined. © 1998 Elsevier Science Ltd. All rights reserved

Keywords: persulfurated; crystal structure; fluorothiolates; palladium; platinum; sulfur inversion.

1. INTRODUCTION

The chemistry of co-ordination compounds with metal centres surrounded exclusively by sulfur donor ligands has been extensively examined. The interest in this area is due to its relevance to *i.a.* catalysis, bioinorganics and structural chemistry [1–6].

For complexes containing chiral three co-ordinated sulfur atoms, several structural and kinetic studies have been undertaken with regard to the interconversion of isomers that arises from configuration inversion at the sulfur atoms [7,8].

However, for those complexes with three or more possible NMR-observable conformers [9,10], since there is no conclusive evidence to distinguish among spectroscopic signals arising from different conformers, seldom is a precise assignment accomplished [11–13].

Previously [14–16] we were interested in the chemistry of metal centres surrounded exclusively by sulfur atoms and as part of the research done, in this paper we report the syntheses of $[M(SR_F)_2(CH_3SCH(CH_3)CH(CH_3)SCH_3)]$, M = Pd, $SR_F = SC_6F_5$, **1**; $SR_F = SC_6RH$-4, **2**; M = Pt, $SR_F = SC_6F_5$, **3**; $SR_F = SC_6F_4H$-4, **4**; the separation of two sets of isomers for each complex and the X-ray diffraction crystal structure of a diastereomer of $[Pt(SC_6F_5)_2(CH_3SCH(CH_3)CH(CH_3)SCH_3)]$. The separation of both diastereomers allows, for the first time, a direct identification of the stereoisomers present in solution by ^1H, ^{19}F and ^{195}Pt NMR.

2. EXPERIMENTAL

$[MCl_2\{(meso, rac)\text{-}CH_3SCH(CH_3)CH(CH_3)SCH_3\}]$, M = Pd or Pt [17], $Pb(SC_6F_5)_2$ [18] and $Pb(SC_6F_4H\text{-}4)_2$ [19] were prepared according to published methods.

After $[MCl_2\{(meso, rac)\text{-}CH_3SCH(CH_3)CH(CH_3)SCH_3\}]$, M = Pd or Pt (1.2 mmol) and $Pb(SC_6F_5)_2$ or $Pb(SC_6F_4H\text{-}4)_2$ (1.2 mmol) were dissolved in 60 ml of

---

* Author to whom correspondence should be addressed.

acetone, the resulting suspensions were magnetically stirred for 2 h at room temperature. $PbCl_2$ was then filtered off and the clear orange or yellow solutions were evaporated to dryness (yields: **1** = 90%, **2** = 84%, **3** = 96% and **4** = 91%).

0.75 g of silica-gel were added to the solids (*ca.* 0.15 g) after they were dissolved in *ca.* 15 ml of acetone. For each compound, the solvent was evaporated and the impregnated silica was placed on top of a chromatographic column and eluted with chloroform:acetone (10:1) to obtain solutions of *cis* [$R_f = 3.8$, **1**-*cis* (23.5%); $R_f = 3.6$, **2**-*cis* (47.9%); $R_f = 3.1$, **3**-*cis* (41.3%); $R_f = 3.0$, **4**-*cis* (43.2%)] and *trans* [$R_f = 4.9$, **1**-*trans* (10.9%); $R_f = 4.7$, **2**-*trans* (25.43%); $R_f = 4.4$, **3**-*trans* (48.9%); $R_f = 4.2$, **4**-*trans* (51.8%)] isomers.

Slow evaporation of these solutions at room temperature afforded orange powders or yellow crystals. Analytical data were determined by Galbraith Laboratories, U.S.A.

Infrared spectra were recorded over the 4000–200 cm^{-1} range as CsI pellets on a Perkin-Elmer 1330 instrument equipped with a data station.

^1H, ^{19}F and ^{195}Pt NMR spectra were measured with a SDS-360 MHz and a modified NT-360 spectrometer operating at 360, 282.23 and 77.1 MHz, respectively, by Spectral Data Services (IL, U.S.A.). Chemical shifts are relative to TMS, $\delta = 0$ (^1H); $CFCl_3$, $\delta = 0$ (^{19}F) and $Na_2[PtCl_4]/D_2O$, $\delta = 0$ (^{195}Pt). A standard variable temperature unit was used to control the probe temperature, which was checked periodically by a thermocouple to ensure that temperature readings were kept within ±1°C. Palladium complexes were studied in $(CD_3)_2CO$ from -37 to 40°C and platinum complexes were studied in $(CD_3)_2CO$ at room temperature and in $(CD_3)_2SO$ at high temperatures.

Crystallographic data for $[Pt(SC_6F_5)_2(CH_3SCH(CH_3)CH(CH_3)SCH_3)]$ **3**-*cis*: $C_{18}H_{14}F_{10}PtS_4$, $M = 743.61$, $a = 7.102(1)$, $b = 19.066(3)$, $c = 16.799(3)$ Å, $\beta = 94.71(2)°$, $U = 2267.0(6)$ Å^3, $T = 295$ K, space group $P2_1/n$, $Z = 4$, $\rho = 2.179$ g cm^{-3}, $\mu = 66.93$ cm^{-1}. A crystal of dimensions $0.17 \times 0.12 \times 0.18$ mm was used for indexing and intensity data collection in the scan mode by using graphite monochromatized Mo-Kα radiation in a Siemens AED diffractometer using $\omega/2\theta$ scans ($3 \leq 2\theta \leq 50°$). They were corrected for Lorentz, polarisation and absorption effects. The structure was solved by the Patterson method. All non-hydrogen atoms were anisotropically refined (SHELX-76) [20] and hydrogen atoms were included in the observed positions. Final R and R_w values were 0.024 for 3171 observed reflections [$F \geq 5\sigma(F)$].

3. RESULTS AND DISCUSSION

Methathetical reactions of $[MCl_2\{(meso, rac)\text{-}CH_3SCH(CH_3)CH(CH_3)SCH_3\}]$, M = Pd or Pt with the anionic pseudohalogens $(SC_6F_5)^-$ or $(SC_6F_4H\text{-}4)^-$ in acetone proceeded as expected to give $[M(SR_F)_2\{(meso, rac)\text{-}CH_3SCH(CH_3)CH(CH_3)SCH_3\}]$, M = Pd, $SR_F = SC_6F_5$, **1**; $SR_F = SC_6F_4H\text{-}4$, **2**; M = Pt, $SR_F = SC_6F_5$, **3**; $SR_F = SC_6F_4H\text{-}4$, **4**; as orange–red (**1** and **2**) or yellow crystalline (**3** and **4**), air stable complexes which are soluble in acetone and dichloromethane. Analytical data consistent with the given formulation have been deposited as supplementary data.

Infrared spectra show characteristic absorption bands of the fluorinated moieties: 1515, 1480, 1085, 975 and 855 cm^{-1} for $SR_F = SC_6F_5$ and 1480, 1430, 1165 and 910 cm^{-1} corresponding to $SR_F = SC_6F_4H\text{-}4$ [19]. Other infrared frequencies agree with the dithiolate ligand expected absorptions, but have been omitted since they are of limited value to the following discussion.

From each compound **1** to **4**, two isomers were separated by dry column chromatography on silica-gel by using a chloroform–acetone mixture as eluent as described in Section 2.

Single crystals of the **3**-*cis*, were isolated by slow evaporation of chloroform:acetone solutions at room temperature. The X-ray diffraction structure of **3**-*cis* is shown in Fig. 1 and selected geometric data are collected in Table 1.

The molecules exhibit a slightly distorted square-planar arrangement around the platinum centre, with four co-ordinated sulfur atoms showing a clear sp^3 hybridisation. The racemic mixture of the *cis* isomer crystallise as the conformer with a formal alternate chiral configuration, *RSRS* or *SRSR*, in the chiral atoms of the chelated thioether ligand $CH_3SCH(CH_3)CH(CH_3)SCH_3$. The molecular structure of **3**-*cis* corresponds to isomer **A** (see Fig. 4 below).

Sharp *et al.* [21] have found a closely related structure for $[PtCl_2(CH_3SCH(CF_3)CH(CF_3)SCH_3)]$ in which the trifluomethyl groups lie on the opposite side of the chelate ring from the methyl substituents.

The observed mean values for the Pt–S (Pt–SR_F 2.317 and Pt–SC_2 2.291 Å) and S–C [S–C(sp^2) 1.765 and S–C(sp^3) 1.817 Å] bond distances are similar to those found on the related *trans*-$[Pt(SC_6F_5)(SEt_2)_2]$ [16] [Pt–SR_F 2.323, Pt–SC_2 2.302; S–C(sp^2) 1.760, S–C(sp^3) 1.808 Å].

For $[PtCl_2(CH_3SCH(CF_3)CH(CF_3)SCH_3)]$ [21] the platinum–sulfur mean distance is slightly shorter (Pt–SC_2 2.237 Å) probably reflecting a lower *trans*-influence of the chloride ligand as compared with that of the $SC_6F_5^-$ moiety [22]. In general, sulfur–carbon lengths agree satisfactorily with the ranges described for this type of bond distance [23].

The isomers separated from these complexes can be explained simply in terms of the relative orientation of the substituents on methine groups (*cis* and *trans* diastereomers). As shown in Fig. 2, the ring is puckered at the carbon atoms but, as is the case with five membered rings at room temperature, there is fast ring inversion in all species investigated to date. At low temperature, however, few conformers have been previously identified in solution [17].

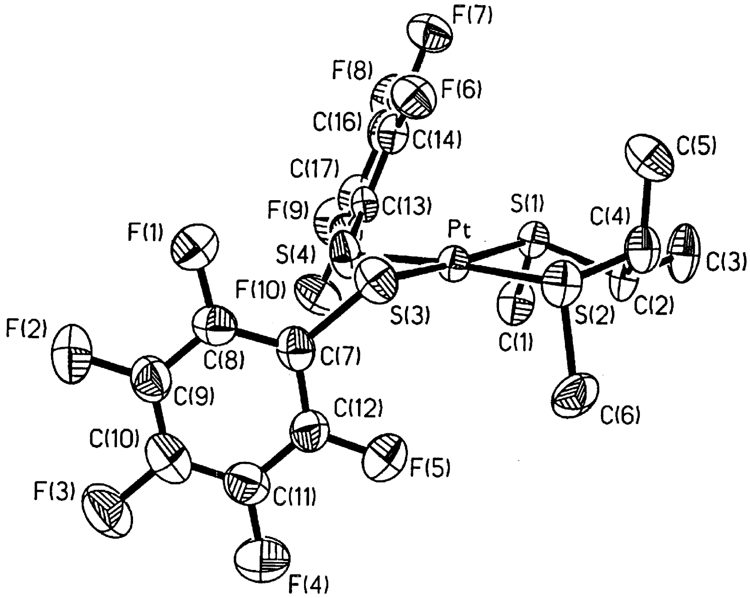

Fig. 1. X-ray structure of $[Pt(SC_6F_5)_2(CH_3SCH(CH_3)CH(CH_3)SCH_3)]$, **3**-*cis*.

Table 1. Selected molecular dimensions (bond lengths in Å, angles in °) for $[Pt(SC_6F_5)_2(CH_3SCH(CH_3)CH(CH_3)SCH_3)]$ **3**-*cis* with e.s.d.s. in parentheses

Pt–S(1)	2.293(1)	Pt–S(2)	2.289(1)
Pt–S(3)	2.323(1)	Pt–S(4)	2.310(1)
S(1)–C(1)	1.806(5)	S(1)–C(2)	1.839(5)
S(2)–C(4)	1.827(6)	S(2)–C(6)	1.797(6)
S(3)–C(7)	1.761(5)	S(4)–C(13)	1.768(5)
S(3)–Pt–S(4)	89.95(5)	S(2)–Pt–S(4)	173.76(5)
S(2)–Pt–S(3)	84.81(5)	S(1)–Pt–S(4)	96.93(5)
S(1)–Pt–S(3)	171.56(5)	S(1)–Pt–S(2)	88.59(5)
Pt–S(1)–C(2)	102.63(2)	Pt–S(1)–C(1)	110.70(2)
Pt–S(2)–C(6)	104.81(2)	Pt–S(2)–C(4)	103.35(2)
Pt–S(3)–C(7)	108.83(2)	Pt–S(4)–C(O)	110.97(2)

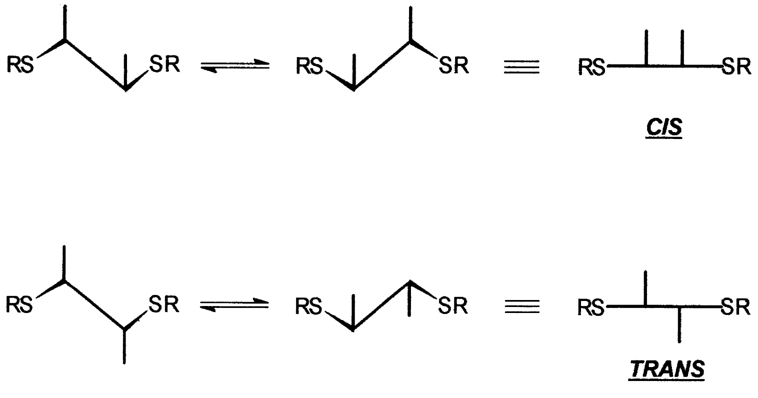

Fig. 2. Diagram representing compounds $[M(SR_F)_2(CH_3SCH(CH_3)CH(CH_3)SCH_3)]$. The $M(SR_F)_2$ unit lies perpendicular to the paper and in the plane defined by the sulfur atoms.

NMR spectra of compounds *cis* and *trans* revealed the expected presence of further isomeric forms arising from the relative position of the methyl substituents on the sulfur atoms with respect to the plane of the metal co-ordination, giving rise to *anti* and *syn* isomers, as exemplified in Fig. 3.

Anti and *syn* conformers can undergo an interconversion process through inversion of configuration at the sulfur centers. These conformational changes of the sulfur substituents are slow enough as to be detected by NMR experiments.

All together, the relative orientations of both sulfur and carbon substituents can, therefore, generate two different sets of non-interconvertable isomers (*cis* and *trans*) with three NMR-detectable and interconvertable conformers in each set, as shown on Fig. 4.

Therefore, in terms of NMR spectroscopy, both methyl substituents on the sulfur atoms (CH_3–S) are equivalent in isomers **A**, **C**, **D** and **F**, whereas isomers **B** and **E** bear pairs of magnetically non-equivalent CH_3–S moieties. Exactly the same is valid when the CH_3–C and R_F–S fragments are considered.

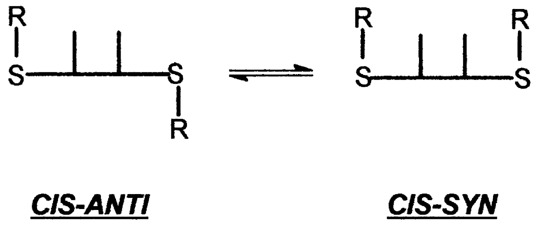

Fig. 3. *Anti* and *syn* isomers of $[M(SR_F)_2(CH_3SCH(CH_3)CH(CH_3)SCH_3)]$.

3.1. *Cis-diastereomers*

NMR selected parameters for compounds **1**-*cis* to **4**-*cis* are collected in Table 2.

^1H NMR spectra of isomers *cis* show three doublets arising from the CH_3–C fragments. In all cases two of these doublets have exactly the same intensity, which suggests that they arise from two non-equivalent methyls attached to the same molecule. These absorptions can, therefore, be assigned unambiguously to isomer **B** in Fig. 4. The third doublet arises from an isomer with magnetically equivalent methyl substituents, which is the case of either **A** or **C**; no definite assignment can be made at this point, however.

Proton NMR spectra also show a complicated overlap of signals due to the -CH–CH- skeleton and, as before, three signals for the CH_3–S substituents which, for compounds **3** and **4**, exhibit satellites characteristic of magnetic coupling with platinum (^{195}Pt, 34% abundance). J_{Pt-H}(**3**-*cis*) = 42.1 Hz and J_{Pt-H}(**4**-*cis*) = 42.1 Hz.

In addition, when $R_F = C_6F_4H$-4 (*cis*-compounds **2** and **4**), three triplets of triplets, characteristic of the X part of two distinct A_2B_2X magnetic systems, are detected.

This fact is of interest and seldom observed since practically all spectroscopic studies on this type of compound focus on the neutral ligand. Very few of the anionic ligands used before are suitable for NMR observation. The fluorothiolates involved in this work thus allow the distinction between magnetic non-equivalence brought up by the molecular asymmetry.

The presence of distinguishable thiolates is also reflected on the ^{19}F NMR spectra, showing three doublets for the *ortho*-fluorine atoms, a complicated multiplet of overlapping signals due to *meta*-fluorine

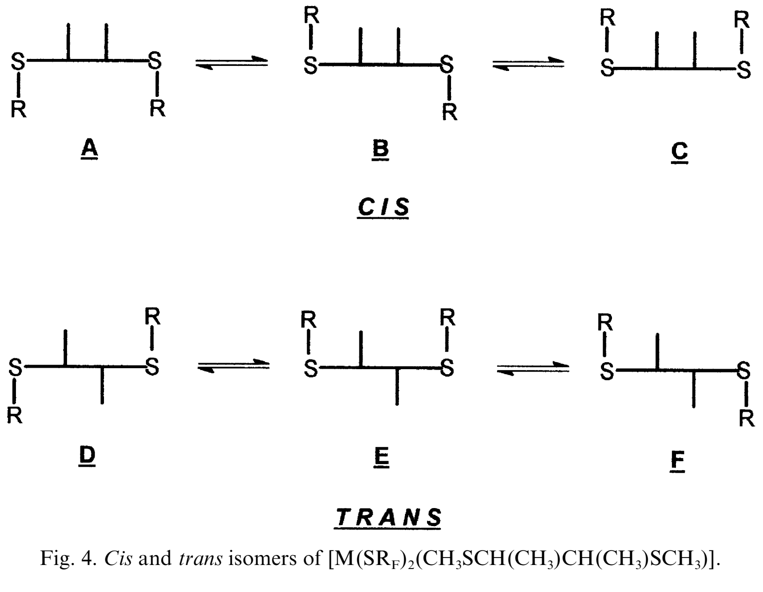

Fig. 4. *Cis* and *trans* isomers of $[M(SR_F)_2(CH_3SCH(CH_3)CH(CH_3)SCH_3)]$.

Table 2. NMR selected parameters for *cis*-diastereomers of $[M(SR_F)_2(CH_3SCH(CH_3)CH(CH_3)SCH_3)]$ **1**–**4**, M = Pd, $(CD_3)_2CO$ at 237 K; M = Pt, $(CD_3)_2CO$ at 298 K

	δ's				J's		
	Pt	H_p	F_o	F_p	$^3J_{Fo}-F_m$	$^3J_{Fm}-F_p(H)$	$^4J_{Fo}-F_p(H)$
1							
A			−131.95d	−162.03t	27.9	20.4	–
B			−132.30d	−162.63t			
			−132.63d	−162.65t			
2							
A		7.30tt	−132.73m		–	10.2	7.5
B		7.28tt	−133.06m				
		7.31tt	−133.27m				
3							
A	−4253s		−130.91dd	−161.34tt	28.0	21.3	7.9
B	−4251s		−131.16dd	−161.64t			
			−131.42dd	−161.76t			
4							
A	−4340s	7.07tt	−132.62m		–	10.3	7.2
B	−4339s	7.06tt	−132.88m				
		7.08tt	−133.77m				

atoms and, for complexes **1** and **3**, three triplets arising from the fluorine atoms in the *para* position of the fluorinated ring [Fig. 5(a)].

This spectroscopic information is consistent with the presence of only two out of the three, **A**, **B** and **C** possible isomers. Considering the multiplicity observed on the NMR signals, isomer **B** can be recognised unambiguously, but a distinction between **A** and **C** (Fig. 4) is not evident.

Further evidence for the presence of a single pair of isomers was able to be gained from ^{195}Pt–$\{^1H\}$ NMR spectra of compounds **3**-*cis* and **4**-*cis* at room temperature. **3**-*cis* shows two singlets at $\delta_{Pt} = -4253$ and -4251 ppm with a relative proportion of 5.9 to 1. **4**-*cis* shows two absorptions at $\delta_{Pt} = -4340$ and -4339 ppm with 3.5 to 1 relative intensities.

Molecular models indicate extensive steric interactions between the sulfur and carbon substituents and they appear to be in the order **A** < **B** < **C**. In agreement with this order in which the least hindered isomers are predicted to have equivalent methyl–sulfur substituents, it is reasonable to assume that the most abundant isomer is **A**, while **C** has the lowest, unobservable, concentration. Assignment of signals at $\delta_{Pt} = -4253$ (**3**-*cis*) and -4340 (**4**-*cis*) ppm to isomers **A** rather than to isomers **C**, seems further supported by the fact that the structure found in the solid state for $[Pt(SC_6F_5)_2(CH_3SCH(CH_3)CH(CH_3)SCH_3)]$ is in fact that of isomer **A**.

According to that assignment, the relative population of isomers **A** and **B** (Fig. 4), for compounds **1** to **4**, are given in Table 3.

3.2. *Trans-diastereomers*

NMR selected parameters for compounds **1**-*trans* to **4**-*trans* are collected in Table 4.

^1H NMR spectra of complexes *trans* show a complex, ill-defined multiplet on the CH_3–C region. Four signals, however, arising from the CH_3–S fragments, were clearly observed.

For compounds **3** and **4**, these signals exhibit satellites characteristic of ^1H–^{195}Pt magnetic coupling with platinum (^{195}Pt, 34% abundance). J_{Pt-H}(**3**-*trans*) = 41.4 Hz and J_{Pt-H}(**4**-*trans*) = 42.5 Hz.

For all compounds **1** to **4**, two of these signals have exactly the same intensity, suggesting that they arise from two non-equivalent methyls attached to the same molecule. These absorptions can, therefore, be assigned unambiguously to isomer **E** in Fig. 4. The remaining two signals are resonances from isomers **D** and **F**, both having magnetically equivalent methyl substituents.

Proton NMR spectra also display a complex multiplet of overlapping signals due to the -CH–CH- skeleton. In addition, when $R_F = C_6F_4H$-4 (*trans*-compounds **2** and **4**), four signals characteristic of the X

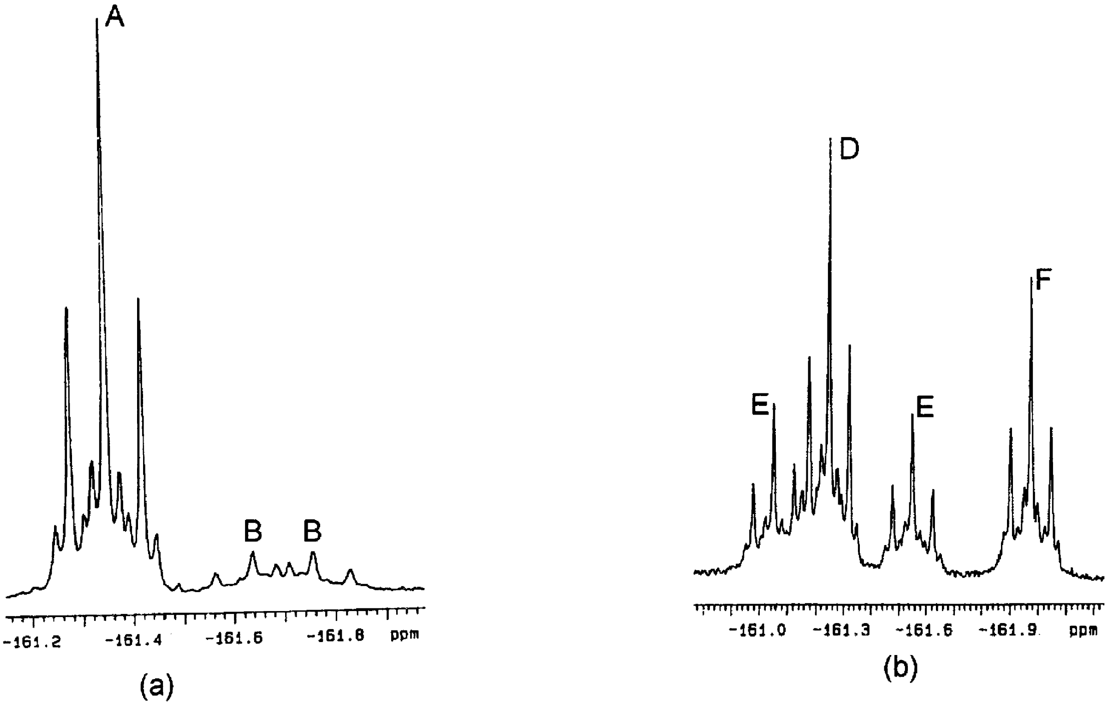

Fig. 5. ^{19}F NMR of *para*-fluorine region of $[Pt(SC_6F_5)_2(CH_3SCH(CH_3)CH(CH_3)SCH_3)]$ **3**-*cis* (a) and **3**-*trans* (b).

Table 3. Relative isomeric populations for $[M(SR_F)_2(CH_3SCH(CH_3)CH(CH_3)SCH_3)]$, M = Pd (237 K), $R_F = C_6F_5$ **1**; C_6F_4H-4 **2**; M = Pt(298 K), $R_F = C_6F_5$ **3**; C_6F_4H-4 **4**

	Cis			*Trans*		
	A	B	C	D	E	F
1	6.3	1	–	1.1	1.4	1
2	5.6	1	–	1.1	1.3	1
3	5.9	1	–	1.3	1.1	1
4	3.5	1	–	1.2	1.1	1

part of three different A_2B_2X magnetic systems, are detected.

^{19}F NMR spectra show four doublets for the *ortho*-fluorine atoms, a complicated multiplet of overlapping signals due to *meta*-fluorine atoms and, for complexes **1** and **3**, four triplets of triplets arising from the fluorine atoms in the *para* position of the fluorinated ring [Fig. 5(b)]. No ^{19}F–^{195}Pt magnetic couplings were observed.

The available spectroscopic information is consistent with the presence of isomers **D**, **E** and **F** (Fig. 4) in solution of compounds **1**-*trans* to **4**-*trans*.

Further evidence of such an isomeric distribution is gained from ^{195}Pt–$\{^1H\}$ NMR spectra of compounds **3**-*trans* and **4**-*trans* which show, at room temperature, three singlets at $\delta_{Pt} = -4252$, -4257 and -4261 ppm and $\delta_{Pt} = -4339$, -4342 and -4343 ppm, respectively. The relative intensities of these signals are 1.3:1.1:1 for **3**-*trans* and 1.2:1.1:1 for **4**-*trans*.

As seen before, molecular models indicate considerable steric interactions between the sulfur and carbon substituents, which appear to be in the order **D** < **E** < **F**. In agreement with this order in which the least hindered isomers are predicted to have *anti* and equivalent sulfur substituents, the most abundant isomer is probably **D**, whereas **F** appears to be the least abundant.

The relative populations assigned to *trans*-isomers **D**, **E** and **F** (Fig. 4), for compounds **1** to **4**, are given in Table 3.

Conformers **A** and **B**, on the one hand, as well as **D**, **E** and **F**, on the other, are involved in dynamic equilibria due to a configuration inversion at the thioether sulfur atoms. The pyramidal inversion is a relatively slow process suitable for detection within the NMR time scale as the individual absorptions from each isomer coalesce into a single averaged resonance.

As expected, the thiolate ligands seem to have fast free rotation and, at room temperature and higher, do not participate in the fluxionality of these molecules.

For comparable compounds, palladium derivatives show lower coalescence temperatures than does platinum. This can be attributed to the more effective 3p(S)–4d(Pd) overlap compared with the 3p(S)–5d(Pt)

Table 4. NMR selected parameters for *trans*-diastereomers of $[M(SR_F)_2(CH_3SCH(CH_3)CH(CH_3)SCH_3)]$ **1**–**4**, M = Pd, $(CD_3)_2CO$ at 237 K; M = Pt, $(CD_3)_2CO$ at 298 K

	δ's				J's		
	Pt	H_p	F_o	F_p	$^3J_{Fo}-F_m$	$^3J_{Fm}-F_p(H)$	$^4J_{Fo}-F_p(H)$
1							
D			−131.87d	−162.19t			
E			−131.78d	−161.75t	27.1	21.0	–
			−131.95d	−162.29t			
F			−132.45d	−162.91t			
2							
D		7.30tt					
			−132.70m				
E		7.29tt			–	10.2	7.5
		7.28tt					
			−133.09m				
F		7.26tt					
3							
D	−4252s		−130.88dd	−161.26tt			
E	−4257s		−130.80dd	−161.05tt	28.2	22.6	8.5
			−130.92dd	−161.55tt			
F	−4261s		−131.44dd	−161.98tt			
4							
D	−4339s	7.08tt					
			−132.97m				
E	−4342s	7.06tt			–	10.3	7.2
		7.07tt	−132.57m				
F	−4343s	7.04tt					

overlap, which allows an easier access to the transition state in the case of palladium complexes [24]. In fact, palladium derivatives show slow sulfur inversion at 237 K while platinum derivatives show it at 298 K in $(CD_3)_2CO$ solutions.

For palladium complexes we have measured coalescence temperatures by observing the ^{19}F NMR spectra of the thiolate moieties. For platinum complexes, coalescence temperatures were determined directly from the variable temperature ^{195}Pt NMR spectra. Coalescence temperatures are collected in Table 5.

Cis-compounds **1** to **4** show a single coalescence of signals in agreement with the fast interconversion **A**⇔**B**. On the other hand, *trans*-compounds **1** to **4** give rise to two consecutive temperatures of coalescence, in agreement with a process involving three species: **D**⇔**E**⇔**F** for which two different energies of inversion are reasonably to be expected (Fig. 6).

In summary, NMR studies of each diastereomer of complexes **1** to **4** show the presence of three conformers of the *trans* isomers but only two of the *cis* isomer. In general, NMR spectra are quite similar and only slight changes in the relative isomeric populations were observed. As expected, relative abundances can be detected regardless of the observed nuclei.

Table 5. Coalescence temperatures of the compounds **1** to **4**

Compound[a]	Isomer	CT1[b]	Isomer	CT1[b]	CT2[b]
1 $[Pd(SC_6F_5)_2L]$	*cis*	283	*trans*	283	308
2 $[Pd(SC_6F_4H\text{-}4)_2L]$	*cis*	283	*trans*	283	308
3 $[Pt(SC_6F_5)_2L]$	*cis*	333	*trans*	343	363
4 $[Pt(SC_6F_4H\text{-}4)_2L]$	*cis*	333	*trans*	343	383

[a] $L = CH_3SCH(CH_3)CH(CH_3)SCH_3$.

[b] Coalescence temperature (CT) in K.

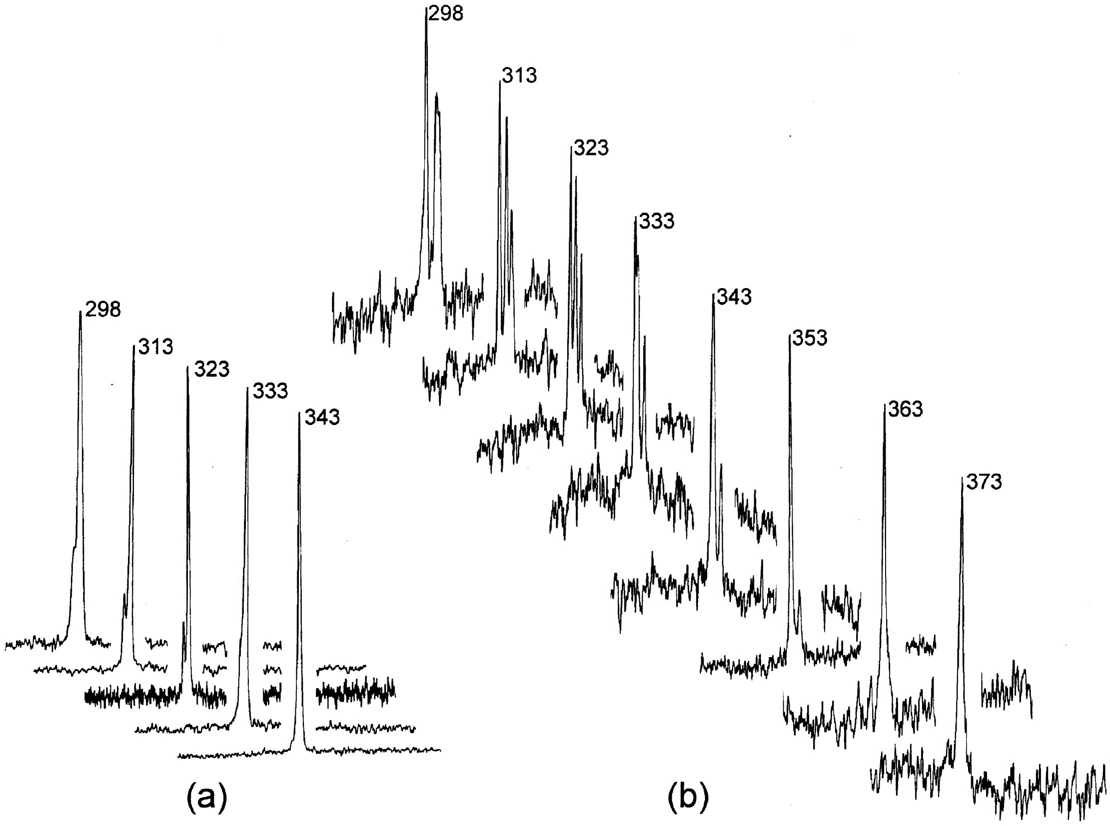

Fig. 6. Variable temperature ^{195}Pt NMR spectra of $[Pt(SC_6F_5)_2(CH_3SCH(CH_3)CH(CH_3)SCH_3)]$ **3**-*cis* (a) and **3**-*trans* (b).

4. SUPPLEMENTARY MATERIAL AVAILABLE

Tables of analytical data are shown in Appendix A. Crystal and intensity measurement data, positional parameters of calculated hydrogen atoms, anisotropic thermal parameters and bond distances and angles have been deposited at Cambridge Crystallographic Data Centre, deposition code: 101590.

Acknowledgements—We wish to thank DGAPA-UNAM, PADEP-UNAM and CONACYT for financial support and to Dr Sylvain Bernès for his helpful assistance.

REFERENCES

1. Stephan, D. and Nadasdi, T., *Coord. Chem. Rev.*, 1996, **147,** 147.
2. Krebs, B. and Henkel, G., *Angew. Chem. Int. Ed. Engl.*, 1991, **30,** 769.
3. Blower, P. and Dilworth, J., *Coord. Chem. Rev.*, 1987, **76,** 121.
4. Black, J. R., Champness, N. R., Levason, W. and Reid, G., *J. Chem. Soc. Dalton Trans.*, 1995, 3439.
5. Black, J. R., Champness, N. R., Levason, W. and Reid, G., *J. Chem. Soc. Chem. Commun.*, 1995, 1277.
6. Black, J. R. and Levason, W., *J. Chem. Soc. Dalton Trans.*, 1994, 3225.
7. Abel, E. W., Bhargava, S. K. and Orrell, K. G., *Prog. Inorg. Chem.*, 1984, **32,** 1.
8. Orrell, K. G., *Coord. Chem. Rev.*, 1989, **96,** 1.
9. Orrell, K. G., Šik, V., Brubaker, C. and McCulloch, B., *J. Organomet. Chem.*, 1984, **276,** 267.
10. Abel, E. W., Khan, R., Kite, K., Orrell, K. G. and Šik, V., *J. Chem. Soc. Dalton Trans.*, 1980, 1175.
11. Abel, E. W., Coston, T. P., Higgins, K. M., Orrell, K. G., Šik, V. and Cameron, T. S., *J. Chem. Soc. Dalton Trans.*, 1989, 701.
12. Abel, E. W., Moss, I., Orrell, K. G., Šik, V., Stephenson, D., Bates, P. A. and Hursthouse, M. B., *J. Chem. Soc. Dalton Trans.*, 1988, 521.
13. Mao, X.-A., Yao, J.-Z., Tian, B.-S. and Chen, Y.-Y., *Magn. Reson. Chem.*, 1996, **34,** 109.
14. Cruz-Garritz, D., Leduc, B., López-Tercero, J., Martin, E. and Torrens, H., *Rev. Soc. Quim. Méx.*, 1990, **34,** 76.
15. García, J., Martin, E., Morales, D., Torrens, H. and Del Río, F., *Inorg. Chim. Acta*, 1993, **207,** 93.
16. Cruz-Garritz, D., Martin, E., Torrens, H. and Mayoh, K., Smith, A., *Trans. Met. Chem.*, 1991, **16,** 236.
17. Cross, R. J., Rycroft, D. S., Sharp, D. W. A. and Torrens, H., *J. Chem. Soc. Dalton Trans.*, 1980, 2434.

18. Peach, M. E., *Can. J. Chem.*, 1968, **46,** 2699.
19. Bertran, A., Garcia, J., Martin, E., Sosa, P. and Torrens, H., *Rev. Soc. Quim. Mex.*, 1993, **37,** 185.
20. Sheldrick, G. M., *SHELX Systems Report*. University of Cambridge, 1976.
21. Hunter, W. N., Muir, K. W. and Sharp, D. W. A., *Acta Cryst. C*, 1984, **40,** 37.
22. Cruz-Garritz, D., Chamizo, J. A., Cruz, M. and Torrens, H., *Rev. Soc. Quim. Mex.*, 1989, **33,** 18.
23. Orpen, A. G., Brammer, L., Allen, F. H., Kennard, O., Watson, D. G. and Taylor, R., *J. Chem. Soc. Dalton Trans.*, 1989, 31.
24. Abel, E. W., Evans, D. G., Koe, J. R., Šik, V., Bates, P. A. and Hursthouse, M. B., *J. Chem. Soc. Dalton Trans.*, 1989, 985.

APPENDIX A

SUPPLEMENTARY ANALYTICAL DATA

The analytical data of **1**–**4** *meso*/*rac*-complexes are given in Table 6. The analytical data of *cis* and *trans* complexes are given in Table 7.

Table 6. Analytical data of **1**–**4** *meso*/*rac*-complexes

Compound[a]	Analyses (%)[b]		
	C	H	S
1 [Pd(SC_6F_5)$_2$L]	32.6 (33.0)	2.3 (2.2)	19.2 (19.6)
2 [Pd(SC_6F_4H-4)$_2$L]	34.4 (34.9)	2.8 (2.6)	20.4 (20.7)
3 [Pt(SC_6F_5)$_2$L]	28.9 (29.1)	1.7 (1.9)	17.3 (17.3)
4 [Pt(SC_6F_4H-4)$_2$L]	30.1 (30.6)	2.4 (2.3)	17.9 (18.1)

[a] L = $CH_3SCH(CH_3)CH(CH_3)SCH_3$.
[b] Calculated values in parentheses.

Table 7. Analytical data of *cis* and *trans* complexes

Compound[a]	Analyses (%)[b]		
	C	H	S
1-*cis* [Pd(SC_6F_5)$_2$L]	32.8 (33.0)	2.3 (2.2)	19.5 (19.6)
1-*trans* [Pd(SC_6F_5)$_2$L]	32.9 (33.0)	2.2 (2.2)	19.4 (19.6)
2-*cis* [Pd(SC_6F_4H-4)$_2$L]	34.7 (34.9)	2.6 (2.6)	20.5 (20.7)
2-*trans* [Pd(SC_6F_4H-4)$_2$L]	34.8 (34.9)	2.5 (2.6)	20.8 (20.7)
3-*cis* [Pt(SC_6F_5)$_2$L]	28.9 (29.1)	1.8 (1.9)	17.3 (17.3)
3-*trans* [Pt(SC_6F_5)$_2$L]	29.0 (29.1)	2.0 (1.9)	17.4 (17.3)
4-*cis* [Pt(SC_6F_4H-4)$_2$L]	30.4 (30.6)	2.4 (2.3)	17.9 (18.1)
4-*trans* [Pt(SC_6F_4H-4)$_2$L]	30.5 (30.6)	2.3 (2.3)	18.2 (18.1)

[a] L = $CH_3SCH(CH_3)CH(CH_3)SCH_3$.
[b] Calculated values in parentheses.